



— CLNS-97-1529

November 21, 1997

CLNS 97/1529

LASER ACCELERATION: A PRACTICAL APPROACH

A Talk presented at LASERS 97, Fairmont Hotel, New Orleans, LA, December 15-19, 1997

A. A. Mikhailichenko

Wilson Laboratory, Cornell University, Ithaca, NY 14850

Ithaca, Cornell, NY, U.S.A.

Abstract

The requirements considered for 2×1 km long linac, driven by a laser radiation distributed within open accelerating structure with special sweeping devices. A 300 J, 100-ps laser flash could provide an accelerating gradient 30 GeV/m for $\lambda \approx 1 \mu\text{m}$ and 3 GeV/m for $\lambda \approx 10 \mu\text{m}$ with the method described. For repetition rate 160 Hz the luminosity associated with colliding beams could reach $L = 10^{30} \text{ cm}^{-2} \text{ s}^{-1}$ per bunch. Multi-bunch operational mode is possible here.

1. Introduction

Very first experimental work on laser acceleration made [1] initiated investigations for a practical implementation of powerful lasers for particle's acceleration. This also moved forward research on laser technology itself [2]. Here we will consider the only methods based on scaling of an accelerating structure down to the laser wavelength. Under this scaling the accelerating structure looks more or less like a grating² and could be filled with electromagnetic field only from the side. This is so called *open* accelerating structure.

Particle acceleration with the grating, excited by a laser field, reviewed once in [3]. Typically, a high intensity laser radiation illuminates *all the grating* along the particle's trajectory. So, illumination of every point of the grating lasts for a time, what is required for a particle to cross the grating. In contrast, the method developed in [4] uses a laser radiation focused into a spot on a grating with a size much smaller, than longitudinal and transverse dimension of the grating. Special sweeping device moves this focal spot in longitudinal direction so, that this spot is following the particle in its motion along the accelerating structure (Traveling Laser Focus, TLF-method). Due to this arrangement, all impulsive laser power acting for accelerating field generation at the instant particle's location only, thereby reducing total power, required from the laser. The power reduction and shortening the illuminating time for every point of the structure is numerically equal to the number of resolved spots, associated with the sweeping device.

2. The method

Fig. 1 describes the idea [4]. The pulse of laser radiation lasts for a time τ , so it has the length $= c\tau$, pos. 1 in Fig. 1. The deflecting device 4 is positioned at the distance R from open structure (grating) 6. Beam of particles 5 is going inside this structure with velocity V . The laser bunch positions in three different times are numbered by 1, 2 and 3. The grating 6 has a length L in longitudinal direction. Device 4 is electrically driven by

electrical pulse for sweeping the laser beam in longitudinal direction synchronously with the particle's passage. Full angle of deflection is $\Theta \approx L/R$. As the deflection lasts for a time τ also, that means that the angular velocity of the light spot on the surface of the grating is $\Omega \approx L/(R\tau)$. At the moment, when the laser bunch arrives at the grating, it has an angle α with respect to the particle's trajectory. Evidently,

$$\theta \cdot \tan \alpha = \frac{cL}{VR}. \quad (1)$$

For electrons or positrons, velocity V is close to the speed of light, so $\alpha \approx \pi/4$.

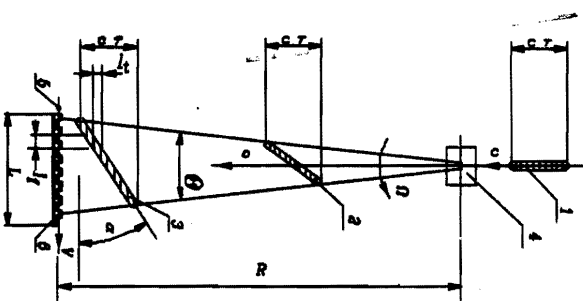


Fig. 1. The principle. The numbers 1, 2 and 3 are numbering the light burst positions in three different moments of time. The length of the laser burst is $c\tau$. 4— is a sweeping device. 5— is the particles' beam, what is going through the structure (grating) 6. The lines across laser bunch show the wavefronts. This is a single accelerating module. l_1 and l_2 are the cross sections of the bunch in longitudinal and transverse directions correspondingly. Each point on the structure illuminated on time $= l_i/c$.

Electric field in each point of the laser beam (pos. 2, 3) polarized rectangularly to the line, connecting this point with the center of the sweeping device 4. With the other words—the wavefronts have common center of curvature coincident with effective center of the sweeping device, see Appendix for more details.

¹ Phone: (607) 255-5253, Fax: (607) 255-8062, e-mail "mikhail@lns2.lsa.cornell.edu"
² We will use both terms — the grating and the accelerating structure.

DEC 22 1997

In Fig. 2 an assembly of such accelerating modules are shown. Here the laser bunch 1 passed through splitting devices 7 generated the secondary bunches 2-4. Sweeping device marked by 9, 8 are the particle's beam focusing elements. The last elements are the same as in Fig. 1. All deflecting elements are synchronized so that the bunch 5 has continuous acceleration in all sections. Distance R and elementary length L defined by technical properties of deflecting device 7 to scan the light beam. As the secondary bunches are generated by the same primary laser bunch (1 in Fig. 2), the longitudinal position for each module does not influence to the accelerating process. In Fig. 1 and Fig. 2 some optical elements necessary for focusing the laser radiation are not shown for simplicity, see lower.

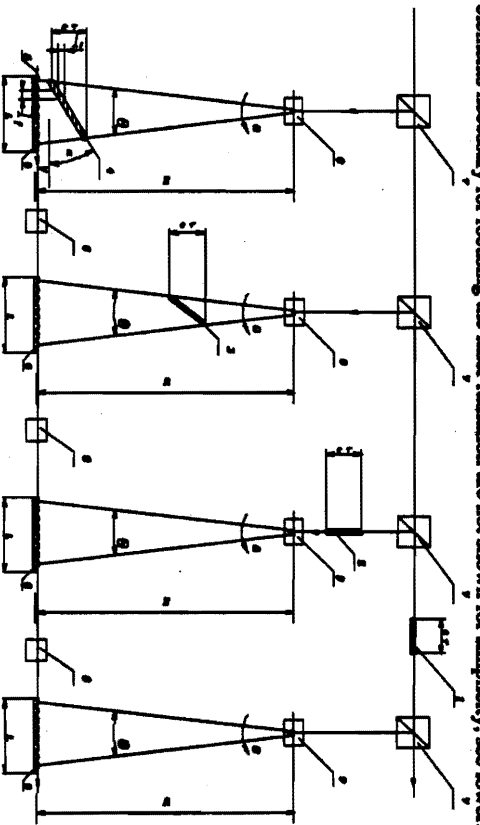


Fig. 2. Accelerating complex. 9— are deflecting devices, 8— particles' beam focusing elements, 7— are the splitters. The last elements are the same as in Fig. 1.

So one can conclude, that parameters of deflecting device are crucial for TLF method. Below we start with description of possible realizations for such devices.

3. The deflecting device

The ratio of deflection angle θ to diffraction angle $\theta_d \approx \lambda/a$, where a is an aperture of the deflecting device, is a fundamental measure of the quality for any deflecting device. This ratio defines the number of resolved spots (pixels), $N_s = \theta/\theta_d$. The deflection angle could be increased by some optics, but the number of resolved spots N_s is an invariant under such transformations. As we mentioned above, N_s value gives the number for the lowering the laser power for gradient desired and, also, the number for reducing the duty time for the structure heating.

Electro-optical devices use controllable dependence of refractive index on electrical field strength and direction applied to some crystals [5-8]. The change of reflecting index is

equal to $\Delta n \approx (\partial n / \partial E) E(t)$. As the refractive index n as a function of applied electric field has a form $1/n_i^2 = 1/n_0^2 + r_{ij} \cdot E_j^2$, where r_{ij} are the components of Electro-optical 6×3 tensor, then $\partial n_i / \partial E_j \approx -n_i^3 \cdot r_{ij} / 2$. Index 4 stands for xz , 5 for xz and 6 for xy .

For a deflecting device based on a prism, Fig. 3, a change in deflecting angle is defined by the phase delay differences at the opposite sides of the laser beam arising from differences in the path lengths in material of the prism

$$\Delta \theta \approx \Delta n \frac{(L_2 - L_1)}{w}, \quad (2)$$

where w is the width of incident light beam, L_1 and L_2 are the distances through which the edges of the light beam traverse the prism, Fig. 1. Basements of the prism are covered by metallization, see Fig. 3. When a voltage $V(t)$ applied to the metallization changes, the refractive index also changes $\Delta n = \Delta n(V(t))$, what yields the change (2) in deflection angle. For such a sweeping device, a lot of electro-optical crystals can be used. For example, a crystal *KDP* (KH_2PO_4) is transparent for a radiation with $\lambda = 0.2 - 1 \mu m$. Some other crystals, such as *CATe*, *CuCl*, *GaAs*, *ZnTe*, *ZnS* are transparent in the region of wavelengths around $1 - 10 \mu m$. The last group of materials have rather high refractive indices (2-4) what compensate smaller electro optical coefficient.

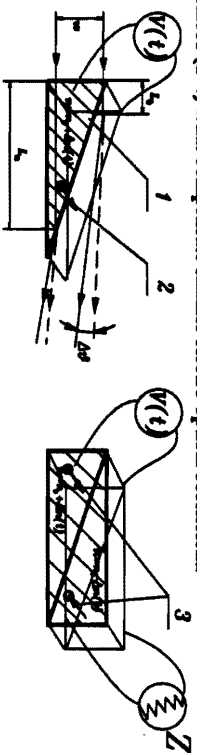


Fig. 3. The prism deflection device concept. Electro-optical crystal prism has a metallization 1 (hatched) on both basements of the prism. Optical axis direction shown by 2. Time dependent voltage applied to metallization.

On the right side two prisms have oppositely-oriented optical axes 3 with the same polarity of electrical field applied. Z is an electrical matching impedance for the voltage supply.

The number of resolvable spots for this device N_s can be found as

$$N_s \approx \frac{\Delta \theta}{\lambda/a} = \frac{\Delta n \cdot (L_2 - L_1) \cdot a}{\lambda w} \approx \Delta n \frac{l}{\lambda}, \quad (3)$$

where $l = L_2 - L_1$ stands for the prism base length and $a/w = 1$ in our case. Substitute for example the numbers for *ZnTe* (transparent for *CO2* laser radiation) which has $n_o = 2.9$, $r_{41} \approx 4.4 \cdot 10^{-12} m/V$, $E \approx 10 kV/cm \approx 10^6 V/m$ one can obtain $\Delta n \approx 10^{-4}$. For *KTN* (Potassium Tantalate Nickel) crystal $\Delta n \approx 7 \cdot 10^{-3}$ for $\lambda \approx 0.63 \mu m$ is possible [8]. Anyway, the shorter wavelength is preferable from this point of view. One can see from (1) and (2) that with the increase in optic path difference both the deflection angle and the

number of resolved spots increase also. To increase the last numbers, *multiple-prism* deflectors were developed, see Fig. 4. We added a *traveling wave* regime here to be able to deflect short light bunches. The plates are wider, than the prisms in transverse direction for uniform field generation in the volume of crystals. Some electrostatic optimization is possible.

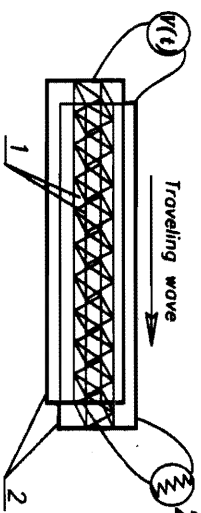


Fig. 4. Prisms 1 with oppositely directed optical axes installed in series between two parallel plate electrodes 2. To be able to deflect short light bunches, the voltage pulse is propagating along the plates (as along a transferring line) as a *traveling wave*. Z is the matching impedance for the transferring line.

One can see that the deflection angle and the number of resolved spots become now

$$\Delta\theta \approx \Delta n \frac{2L_L}{w}, \quad N_s \approx \Delta n \frac{2L_L}{\lambda} \quad (3)$$

where L_L stands for full length of deflecting device. For the previous numbers with $L=30\text{cm}$, one can expect for $w \approx 1\text{cm}$, that deflection angle is $\Delta\theta \approx 10^{-3}$ and $N_s \approx 10$ for $\lambda \approx 10\mu\text{m}$ and, correspondingly $\Delta\theta \approx 10^{-2}$ and $N_s \approx 100$ for $\lambda \approx 1\mu\text{m}$. The last figure looks very promising.

We estimated the voltage applied to the crystals as 10 kV. This is really a voltage variation at the distance corresponding to the half light beam length. This variation is traveling with the light beam along the deflecting device. To be able to manipulate with such rapidly changing voltage at cm range spectral frequencies, some technical arrangements are necessary, see Fig. 5.

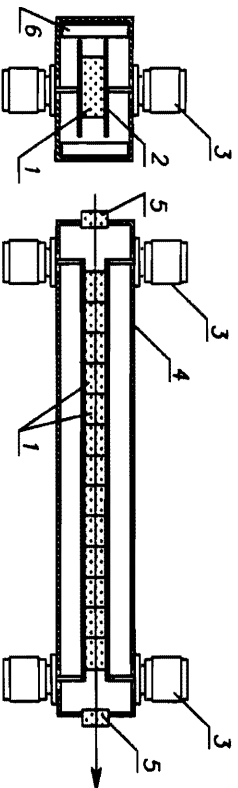


Fig. 5. Arrangement of multi-prism traveling wave deflector. Electro-optical crystals 1 are positioned between plates 2, attached at the end to the

connectors 3. 4—is a cabinet with optical windows 5 from both sides. 6—is a matching dielectric.

Here, basically, a strip-line electrodes 2 have a triangle crystals with opposite optical axes orientation (see Fig.4) in between. A para-phase impulse, applied to one end of strip-line through connectors 3, propagates to the other end and further connected to the matching impedance. So only half of full voltage is applied through each connector. Matching dielectric 6 adjusts the speed of deflecting wave to the speed of light, propagating in crystals. The broad band traveling wave deflector could be obtained also if the same crystals placed in the middle of a waveguide, see Fig.6. There is no difference in principle between these two deflectors. The last one have a bandwidth of a waveguide. Group velocity of electrical wave-pulse must be adjusted to the light velocity in the prisms. Widening of the waveguide helps to reach this goal.

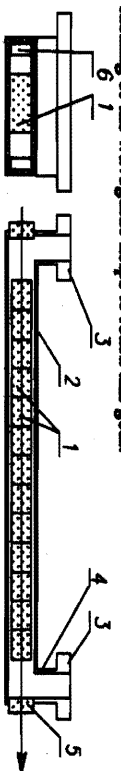


Fig. 6. Multi-prism traveling wave deflector in a waveguide. 1—is electro-optical crystals, positioned in a waveguide 2, having bends 4 with flanges 3. 5—is an optical window. 6 — is a matching dielectric.

A lot of slowly operating devices were routinely in use, see [5]. In [10] for example, the voltage applied about $V = \pm 5\text{ kV}$ provided the deflection angle $\theta = \pm 10^{-3}\text{ rad}$ in KDP device. The device has 10 KDP crystals with total 20 cm length and about 1cm^2 of input aperture.

One can see from (3), that with lowering the cross-section of the laser beam w , the deflection angle could be increased. However, w must be chosen so, that the power density kept below the damage level for this crystal.

In Table 1 we summarized general parameters of electro optical deflectors.

Wavelength	Materials	ϕ , rad	N_s
$\lambda \approx 10\mu\text{m}$	GaAs, ZnTe, ZnS, CaS, CaF ₂ , CaCl	0.01-0.02	10
$\lambda \approx 5\mu\text{m}$	LiNbO ₃ , LiTaO ₃ , CaCl	0.01-0.02	20
$\lambda \approx 1\mu\text{m}$	KDP, DKDP, ADP, KDA, LiNbO ₃	0.01-0.02	100

Table 1

Mechanical deflection system.

Angular frequency of sweeping required is equal $\Omega \approx V/R$, Fig. 1, Fig. 2. Estimate $R \approx 3\text{m}$, we obtain $\Omega \approx 1 \cdot 10^7\text{ rad/sec}$ for $V = c$. The frequency f_m of mechanical oscillations must be at least $f_m \approx \Omega/2\pi = 15\text{ MHz}$. In principle, a mechanical deflection system with a piezoelectric (a quartz for example) can be used for this purposes³. For

³ Quartz plates, sealed in vacuumed bulbs and operating at 50 MHz are commercially available.

obtaining the deflection angle of $\theta \approx L/R \approx 10^{-2}$, the quartz plates must be arranged in multiple reflection deflector assembly [7]. For operation with this high frequency the quartz plates must be placed in a vacuum and must be thin to reduce the power dissipation in a crystal. Example of such array is represented in Fig. 7. Here the laser radiation propagates along the line 1. A fraction of a power scratched with help of splitters 2. Mirrors 3 made on the surface of quartz plates 4. These plates attached to the grounded basement 5 through intermediate supports 6. 7 - is the particle's beam line direction.

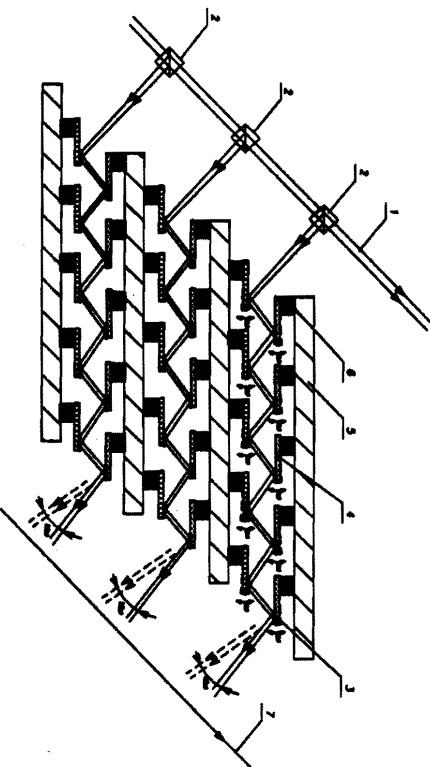


Fig. 7. A mechanical deflecting array. M mirrors 3 ($M = 10$ in Fig. 5) installed on the quartz crystals 4. Resulting deflection angle is M times bigger than with a single mirror. 1 - is a light beam, 7 is a trajectory of a particle's beam. Crystals oscillations phased for a maximal deflection angle.

To optimize deflecting device for maximal number of resolved spots one need to specify the deflection per unit length K . Then the angle inside deflecting device will be $\theta(z) \approx \theta_1 + K \cdot dz$, where θ_1 is an incoming angle. This angle needs to be compared with the angle of divergence $\approx \lambda/w$ what yields $dN \approx \frac{w(z)}{\lambda} K \cdot dz$, where was suggested, that the optical beam width $w(z)$ is a function of distance due to the focusing. Let us suggest also that the plane, where the accelerator structure is located, is a focal one, i.e. $w(z) = w_0 \cdot (F - z)/F$, where F is the distance from the input plane to the focal plane and w_0 is the width on input plane. So one can obtain, that the optimal number of resolved spots is $N_{\text{max}} \approx \frac{w}{\lambda} \cdot \sqrt{Kw}$ and optimal length of deflecting device is $L_{\text{opt}} \approx w \cdot \sqrt{\frac{2}{3Kw}} = \frac{2}{3} F$

[7]. These formulas are valid for any distributed deflection system with the focusing lens installed in front of deflecting device. For a single mirror attached to a piezoelectric, peak-to-peak angular motion $\Delta\theta \approx 8.7 \cdot 10^{-4} \text{ rad}$ is possible [7]. Ten mirrors will give

7

$\Delta\theta \approx 8.7 \cdot 10^{-3} \text{ rad}$, what is acceptable. $N_{\text{max}} \approx \frac{1}{10^{-3}} \cdot \sqrt{8.7 \cdot 10^{-4}} \approx 30$ for $\lambda \approx 10 \mu\text{m}$ and $w \approx 1 \text{ cm}$. For $\lambda \approx 1 \mu\text{m}$, the number of resolved spots will achieve $N_{\text{max}} \approx 300$.

The size of deflecting system in longitudinal direction is limited by sum of the length of accelerating structure and the length of focusing elements. For practical reason the ratio R/a could be $R/a \approx 100$. So the diffraction size of the spot in longitudinal direction could reach $l_s \approx 100\lambda$. The optics can reduce the spot size on the structure and increase the angle of deflection. The number of resolved spots will be the same, however. The value of l_s gives the maximal possible value for Q -factor of the one cell of accelerating structure (see lower).

So, parameters for mechanical deflecting device are about the same as shown in Table 1.

Acousto-optical deflector.

Another possibility to deflect a laser beam is an acousto-optical deflector (see for example [5,11] and references in there). Acoustic wave, induced in a media with piezo-optic effect, provides a cyclic change in the index of refraction with a space period Λ , comparable with the wavelength of radiation. This radiation, having width w crosses the media and gets an angle defined by the Bragg condition, given by $\theta \approx \lambda/\Lambda$. If v stands for acoustic velocity, then $\Delta f \approx v$, where f is a frequency. Effectively changing acoustic wavelength by changing the f during the light pass through the crystal, one can provide the changing in direction of the radiation, passed through this device as

$$\Delta\theta \approx \frac{\lambda}{v} \Delta f \approx \frac{\lambda}{w} \tau \cdot \Delta f, \quad (4)$$

where we recalled the time required for the wave to pass through the light beam width w as $\tau = w/v$ and Δf stands for the range of frequency change. Therefore for the number of resolved spots we obtain [11]

$$N_s \approx \frac{\Delta\theta}{\lambda/w} \approx \tau \cdot \Delta f, \quad (5)$$

so the product of bandwidth and crossing time is crucial for this method. For example for typical velocity $v \approx 0.6 \text{ mm}/\mu\text{s}$, $w \approx 5 \text{ mm}$ the time will be $\tau \approx w/v \approx 5/0.6 \approx 8 \mu\text{s}$. To obtain reasonable number $N_s \approx 20$, one needs to have $\Delta f \approx N_s/\tau \approx 20/8 \approx 2.4 \text{ MHz}$. For increasing the speed of deflection, some sectioning for sound wave excitation need to be done to reduce the effective passing time τ , see [5].

General conclusion for this section is that the light beam deflectors are available with parameters necessary for successful operation. Shorter wavelengths are preferable from the point of maximizing the number of resolved spots. Shorter wavelengths, however, are restricted by the emittances for the particle's beam available (beam must pass through the structure), see lower.

5. Accelerating structure

There are proposals for accelerating structures what could be scaled to match the wavelength of laser radiation [1, 2, 12-14]. Any of these could be used with TFF method. We took the forklake-type structure described in [13] as a basis. This structure looks more advanced due to best possibilities for obtaining vacuum required, alignment and cooling.

8

The *most important* feature, however, is that the boundary grant a good positioning in space to the electromagnetic field map. This reduces a sensitivity to fluctuations in laser beam homogeneity. Structure also gives a good basis for further improvements⁴. We will consider here for a moment the simplest among these types, Fig. 8. Covers 1 adjust the coupling between the groove and outer space. They could be made movable. With this covers the height h is about $h \approx \lambda/2$ and the grooves have inductive coupling with outer space.

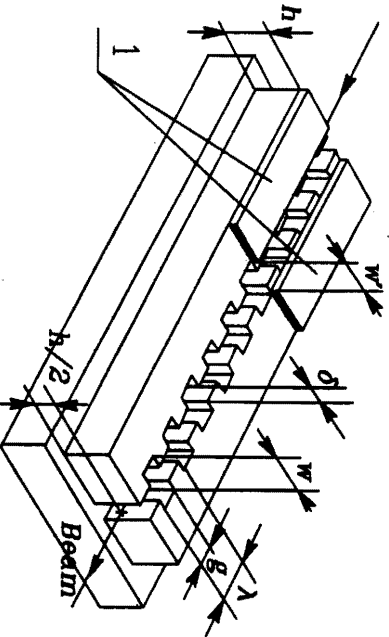


Fig. 8. The forsthole type accelerating structure. Height h is $h \approx \lambda/2$, where λ is a wavelength of incoming laser radiation. $g/\lambda \approx 1/2$, $W \approx 0.7\lambda$, $\delta \approx 0.2\lambda$. 1— are the masks along the structure (cut view) for trimming the coupling (Q_{gr}), $W' \leq W$.

Structure developed in [14] and other one used at Cornell some years ago [15] are very close to this type. The x axes directed across the grating, which has a groove of the width W in this direction (see Fig. 8) and x has a zero in the middle of the slot. The y directed to the depth of the groove and has a zero at the distance $M/2$ from the bottom. The channels for the passing of the beam have a size $\delta \leq 0.2\lambda$. If the width W , g and δ are chosen, the depth of the structure h must be adjusted around $h \approx \lambda/2$. For obtaining necessary electrical coupling of the structure with outer space the masks 1 (Fig. 8) are used. The last defines a quality factor Q_{gr} of the structure. It is clear from the boundary conditions considerations, that as the electrical field on the bottom, $y = -M/2$ is zero, then the variation of electrical field along the y direction must come to zero again. Evidently this happens at the distance $y \approx \lambda_w = h/2$, where λ_w is the corresponding wavelength of radiation in

⁴ The original forsthole structure with open slots in narrow places can accept the field with polarization perpendicular to direction of motion. This yields a systematic modulation of transverse motion. To prevent this one can locate polarization filters on the lens 7, on Fig. 9, see below. Other possibility, to extend the masks over narrower places, marked by dimension δ . More complicated mask profile with horn-type extensions around each groove could be made for accepting the radiation from larger area a for direction it into each individual groove.

the groove, $\lambda_w = \lambda / \sqrt{1 - (\lambda/2W)^2}$. The last formula is exact, if $\delta = 0$. So electrical field, required from boundary condition at the bottom, yields electrical field at orifice also zero, what makes the boundary condition at orifice for incoming radiation looks like a metal. This reduces the field strength at orifice. In original forsthole structure [13] with $h \approx 3\lambda/4$, electrical field reaches the maximum at the orifice and the coupling between the groove and outer space is capacitive. Additional height $\approx \lambda/2$ stores the energy what are not in use. Exact balance of dimensions defines the balance between the power going in the groove and back. Higher value of Q_{gr} reduces the power required from laser to reach the gradient desirable. But most important role this plays in establishment of equilibrium distribution of the field in the structure, preventing a traveling wave regime along y direction. This traveling wave regime occurs in transitory period. The Q_{gr} factor of the order 5-10 could be expected here.

Technological possibilities in lithography are advanced far beyond the requirements associated with this structure scaled down to $\lambda \approx 1\mu m$.

We did intensive calculations for this type of structure with help of GATMIL code [16]. *General conclusion we came to with this structure, is that it is acceptable for acceleration of the particles for the wavelengths $\lambda \approx 1 - 10\mu m$.*

6. A practical scheme

In Fig. 9 there is represented an isometric view from Fig. 2, fulfilled with far or less realistic components, required by TLF method. Coherent radiation generated at central station, travels through splitters 1 aligned in longitudinal direction. Each of secondary beams 2 after passing long focusing lens 3 goes through deflecting devices 4, described in previous section. Polarization of radiation in beams 2 directed along the structure. Further on the way there is a lens 5 for focusing the laser beam in longitudinal direction. After deflection, the laser beam 6 goes through a short focusing cylindrical lens 7. This lens focuses the laser beam on the structure 8 in transverse direction into a spot 9 with a transverse size of a few laser wavelengths. The lenses 3, 5 and 7 produce a small focal point on the grating. In this particular moment, the accelerated particles are located there. The beam is moving along the trajectory 10 and is focused by quadrupoles 11. Each part of the lens 7 is shortly illuminated, so for successful focusing the material with appropriate dispersion must be chosen.

Deflecting voltage must be synchronized with the appearance of the particle's beam in the structure. The focal point 9 is following the beam, *in average*. Some mismatches yield a loss in energy gain only, as the phase of the laser radiation is synchronized once with the particle's beam position. As the driven radiation has the same primary source, all modules could be easily synchronized. The laser focus sweep is limited to the distance about 3cm for practical reasons (see above), so the accelerating device looks like a sequence of 3 cm long accelerating structures with the focusing elements between them.

Different distances to the sweeping device between central and edge parts of the grating (structure), yield a systematic phase shift, what can be easily compensated, however, by variation of the thickness of lens 7 on Fig. 9. Really for a point on the grating, having a longitudinal coordinate s , calculated from the center of the grating, the distance r

between this point and the sweeping device center can be evaluated as $r = \sqrt{R^2 + s^2} \approx R + s^2/2R \approx R + \delta$, what rise a phase variation $\delta\phi \approx 2\pi\delta r/\lambda = 2\pi s^2/\lambda R$. From the other hand, an extra thickness $\Delta(s)$ of the lens provides a phase shift $\delta\phi \approx 2\pi\Delta(s) \cdot (n-1)/\lambda$, where n is refractive index of material of the lens. So, if the thickness variation following the law $\Delta(s) = \frac{s^2}{R \cdot (n-1)}$ (not dependent of λ), then the phase variation will be compensated. Estimation of this value for the end distance $s = 1.5\text{cm}$, $R \approx 3\text{m}$, $n-1 \approx 0.5$, will give $\Delta \approx 23/150\text{cm} = 0.15\text{mm} = 150\mu\text{m}$ only. Some controllable phase variation can be arranged by variation of the lens thickness in longitudinal direction. This required by alternative phase focusing method (APF), see lower. The synchronization of the laser phase and position of the particles yields a transverse force acting to the particle (and what used for effective focusing, see lower).

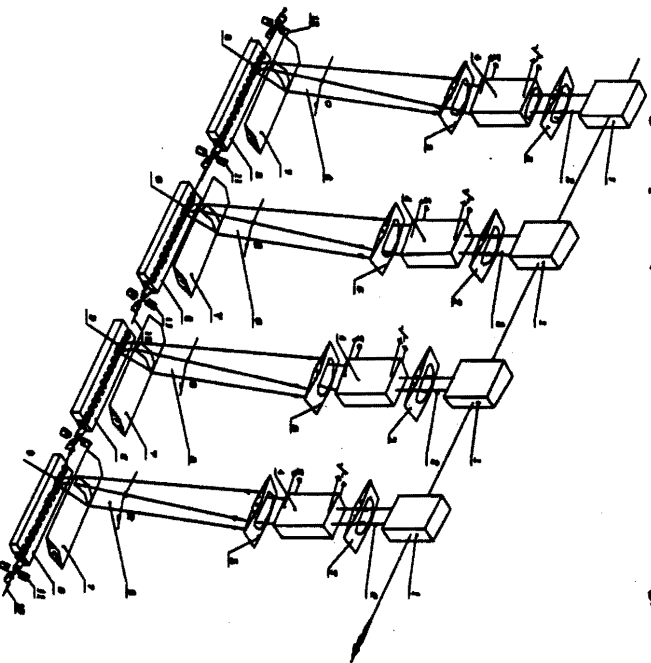


Fig. 9. The Accelerating assembly. This is an isometric view from Fig. 2. Some elements added. Comments are in the text.

A short focusing cylindrical length 7 reduces the transverse size of the spot to a minimal one due to its position close to the accelerating structure. Here the ratio $r/w = 1$, where r is the distance between the lens 7 and the structure 8. The cross section of the laser beam

could be described as $w(y) \approx w(0) \cdot \sqrt{1 + (y/Z_g)^2}$, where $w(0)$ is the waist of the beam at orifice of the groove, y calculated out from the surface of the grating, $Z_g = \pi w^2(0)/\lambda$ is Rayleigh length. Strictly speaking this formula is valid for stationary positioned laser beam, but the properties in transverse direction (what we are interesting in) could be described our conditions as well under. W/c are interesting in regimes, when $w(y) \approx w(0) \cdot (y/Z_g) = y \cdot \lambda/\pi w(0)$. In extreme case $w(0) = \lambda$, we have $w(y) = y/\pi$, so the width of the lens 7 is about the distance between the lens and the structure.

A natural way to increase the deflecting length with the same deflecting angle—is to increase the distance between deflecting device and the accelerating structure. Example of such arrangement is represented in Fig. 10. These arrangements can be very useful for acceleration with laser $\lambda \approx 1\mu\text{m}$, where the number of resolved spots is about 100. This can reduce the total number of deflecting devices (increase L in Fig. 1.2).

Each part of the grating structure is illuminated by duration, which is defined by longitudinal size l , Fig. 1. For example, if we consider $l \approx 100\lambda$, $\lambda = 1\mu\text{m}$, then $l/c \approx 3 \cdot 10^{-9}\text{sec}$. For $\lambda = 10\mu\text{m}$ this value is ten times more. This time is less than the time between electron-electron collisions $\tau = l_{em}/v_e \approx 10^{-10}\text{sec}$, where l_{em} is the free path length, v_e is the electron velocity at Fermi surface [17]. The time of illumination still, however longer, than the time, corresponding to reaction of electron plasmas in metal $\tau \approx 2\pi/\omega_p = 2\pi/\sqrt{4\pi n e^2} = 3 \cdot 10^{-14}\text{sec}$, where n is the density of electrons, r_e is the classical electron radius.

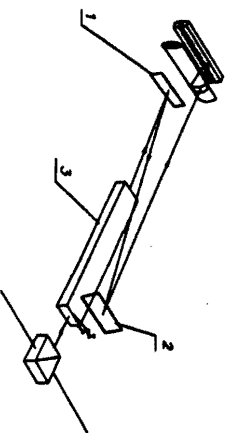


Fig. 10. The way to increase the distance between deflecting device and accelerating structure. 1, 2— are the mirrors, 3— is the deflecting device. Mirrors might be slightly curved to obtain some focusing properties.

So, using a combination of focusing lenses 3, 5, 7 and the sweeping device 4 in Fig. 9, it becomes possible to focus all radiation in a small size on the structure and to move this focal point along the structure in synchronization with instant particle's beam position⁵. After one module passed, the particles go to next module and so on.

7. The injection source

Real beam size defined by its emittance and a focusing applied. To be able to push the beam trough the slots in Fig. 8 with $\delta \approx 0.2\lambda$, beam emittance needs to be rather small.

⁵ Longitudinal length of the particle's beam is a fraction of accelerating wavelength.

Focusing will be considered lower. In this chapter we will investigate the smallest emittances available.

The way to prepare electron or positron beams with low emittance (temperature) was developed in framework of Linear Collider activity. This way uses a damping ring as a cooler. A lot of damping rings were considered for the Linear Collider scheme. They have invariant emittances as low as $(\gamma \epsilon_x) = 3 \cdot 10^{-4} \text{ cm} \cdot \text{rad}$ - radial and $(\gamma \epsilon_y) = 3 \cdot 10^{-4} \text{ cm} \cdot \text{rad}$ - vertical. Energy spread about $\sigma_e \approx 10^{-3}$ and the bunch length $\sigma_z \approx 5 \text{ mm}$. The length of the bunch after one stage compression is of the order $500 \text{ } \mu\text{m}$ and the number of the particles is about $N \approx 10^9$. The second stage compresses the bunch typically to $100 \text{ } \mu\text{m}$ at 10 GeV . So if we need only $N \approx 10^6$, we can loose four orders of magnitude in intensity by *scrapping* the extra particles [4c] ejected from appropriate damping ring, thereby coming to the figures in emittance $(\gamma \epsilon_{x,y}) \approx 10^{-9} \text{ cm} \cdot \text{rad}$. For pre-bunching the FEL mechanism can be used here as well.

The ways to obtain extremely small emittances beyond this value was investigated in [18]. Appropriate to a compact size of Laser Linear Collider complex a *kayak-paddle cooler* is a good candidate [18] for a damping ring. This is basically a damping ring, which made as a sequence of wigglers and RF cavities in straight section, narrowing at a center region for a compacted dimension. The bends can be made to give a small input into cooling process. These arrangements allow to have a dispersion invariant $H_{x,y}$ as small as possible,

$$H_{x,y} = \frac{1}{\beta} \left(\eta_{x,y}^2 + (\beta_{x,y} \eta_{x,y} - \frac{1}{2} R_{x,y} \eta_{x,y})^2 \right) \approx \beta_{x,y} \eta_{x,y}^2, \quad (6)$$

where $\beta_{x,y}$ are envelope functions, $\eta_{x,y}$ are dispersion functions in the wiggler. We have

$$\eta_x = \frac{KR_w}{\gamma} \text{Sin}(s/\lambda_w) = \frac{\lambda_c}{\rho} \text{Sin}(s/\lambda_w), \quad (7)$$

where $\rho = \lambda_w \gamma / K$ is the bending radius in magnetic field of the wiggler, K is the wiggler parameter, $K = eH_1 \lambda_w / mc^2$, λ_w is the wiggler period divided by 2π , H_1 is a transverse magnetic field in the wiggler. This yields the equilibrium invariant emittances as

$$(\gamma \epsilon_x) \approx \frac{1}{2} \lambda_c \hat{A} K^2 \gamma / \rho \approx \frac{1}{2} \lambda_c \hat{A} K^2 / \lambda_w \quad (8)$$

$$(\gamma \epsilon_y) \approx \frac{1}{4} \lambda_c \hat{A} \gamma / \rho \approx \frac{1}{2} \lambda_c \hat{A} K / \lambda_w. \quad (9)$$

where $\lambda_c = h/mc \approx 386 \cdot 10^{-11} \text{ cm}$ is the Compton wavelength.

Substitute here for estimation $\hat{\beta}_{x,y} \approx 1 \text{ m}$, $\lambda_w \approx 5 \text{ cm}$, $K \approx 1$, we obtain

$$(\gamma \epsilon_x) \approx 1 \cdot 10^{-4} \text{ cm} \cdot \text{rad} \quad (8a)$$

$$(\gamma \epsilon_y) \approx 4 \cdot 10^{-9} \text{ cm} \cdot \text{rad} \quad (9a)$$

The beam size defined as

$$\sigma_{x,y} \approx \sqrt{\frac{(\gamma \epsilon_{x,y}) \beta_{x,y}}{\gamma}}. \quad (10)$$

Substitute here radial emittance from (8a) for $\gamma \approx 6000$, 3 GeV , envelope function in laser accelerating structure $\beta \approx 10 \text{ cm}$ (without RF focusing, see lower) one can obtain $\sigma_{x,y} \approx 4 \cdot 10^{-4} \text{ cm} \approx 0.04 \text{ } \mu\text{m}$. 10σ criterion gives the size of hole required for the particle's beam passage as $\delta \approx 10\sigma \approx 0.4 \text{ } \mu\text{m}$. So one can conclude, that only CO_2 laser could be used here. With RF focusing a laser with $\lambda \approx 1 \text{ } \mu\text{m}$ could be used here as well. Number in the beam $N \approx 10^6$ is small enough to be affected by intra-beam scattering.

The Optical Stochastic Cooling (OSC) method [19] could be implemented in the damping ring described above for *further* cooling. This method uses the fluctuations in beam centroid position in a quadrupole wiggler to generate the light with intensity proportional to the number of the particles in the bandwidth. This light interacts after amplification (in optical amplifier) with the same fluctuation in other wiggler. So the optical bandwidth of amplifier allows very fast damping. The amplification coefficient κ of optical amplifier can be expressed as follows

$$\kappa \approx \frac{\epsilon_1}{\epsilon_0} \frac{1}{N} \frac{\Delta f}{f}, \quad (11)$$

where $\epsilon_0 = e^2/mc^2$, $\epsilon_1 = \gamma l \Delta E/E$ is an invariant longitudinal emittance $\Delta f/f$ is a relative bandwidth, N is the number of the particles. One can see that the only phase density in longitudinal direction $\rho_z = q/N$ deals with amplification required. Decrease of emittance after cooling is $\frac{\epsilon_1}{\epsilon_0} \approx \frac{1}{\alpha N}$, where $\alpha = e^2/mc \approx 1/137$, N_e is the number of the particles in the bandwidth, $N_e \approx \frac{f}{\Delta f} N \frac{\lambda_c}{l}$, where l is the bunch length, λ_c is the central wavelength of radiation under amplification. For $N \approx 10^6$, $\lambda_c \approx 10^{-4} \text{ cm}$ ($1 \text{ } \mu\text{m}$), $l \approx 0.01 \text{ cm}$, $\Delta f/f \approx 0.2$ one can expect $N_e \approx 5 \cdot 10^6 \cdot 10^{-2} \approx 5 \cdot 10^4$ and $\epsilon_1/\epsilon_0 \approx 0.01$.

Under this emittance the particle's bunch can be used with the *foxbale-type accelerating structure scaled to* $\lambda \approx 1 \text{ } \mu\text{m}$. To keep the bunch in the kayak-paddle cooler with such a short length, RF cavities must generate an appropriate voltage, because $l \approx \sqrt{qV} < \eta >$, where q is the harmonic number (ratio RF frequency to revolution frequency), V is RF voltage, $< \eta >$ is the dispersion function averaged over the cooler. According to (7) straight section does not give input to $< \eta >$. So a kayak-paddle cooler is a promising compact size machine for preparation the bunch with small emittance.

Other component influence to the beam size in a structure is a focusing system itself. The focusing system includes the quadrupole lenses of appropriate dimensions and a RF focusing.

8. Transverse focusing of particle's beam

Other component influence to the beam size in a structure is a focusing system itself. The focusing system includes the quadrupole lenses of appropriate dimensions and a RF focusing.

* δ is a dimension from Fig. 8

Quadrupole lenses could be placed between the accelerating sections, see Fig.2, 9, 11. This type of focusing was considered in [4c]. The lens focusing parameter can be expressed as

$$\frac{G}{(H\rho)} = k = \frac{\sqrt{2Q} - \cos\mu}{2l(L+2l)} \quad (12)$$

where G is the lens gradient, $(H\rho) \cong pc/300$ is the magnet rigidity of the particle, μ is a betatron tune shift per one period, $2l$ is the length of a quadrupole, L is the distance between lenses, comparable with L from Fig. 1.2. The modulation M of the β -function between the lenses looks like

$$M^2 = \frac{\beta_{\text{min}}}{\beta_{\text{max}}} = \frac{1 + \tanh\phi(\tan\phi + L/l)}{1 - \tanh\phi(\tan\phi + L/l)} \quad (13)$$

$\phi = l\sqrt{k}$ — is the half phase shift in the lens. For $L=4\text{cm}$, $l=0.4\text{cm}$, $\mu = \pi/6$ one can obtain $k \cong 5 \cdot 10^3 1/\text{m}^2$, $\phi^2 = l^2 \cdot k = 2 \cdot 10^3$, and $M^2 \cong 1.5$. For maximal value of the envelope function we have

$$\beta_{\text{min}} \cong M \frac{1}{|H|} \frac{1}{\sqrt{2/3 + L/l}} = \frac{2M \cdot (L+2l)}{\sqrt{2/3 + L/l}} \frac{1}{\sqrt{2/3 + L/l}}$$

which for previous values of L and l gives $\beta_{\text{min}} \cong 15\text{cm}$ and $\beta_{\text{max}} \cong 10\text{cm}$. These values we used above. One can see from (12) that to obtain certain value k [1/m²] for the particles with momentum p [GeV/c], the gradient required is $G \cong 0.3\mu k$. For example, the particles with intermediate momentum $p \cong 10$ GeV/c, $k = 5 \cdot 10^3 1/\text{m}^2$, gradient required is $G \cong 1.5 \cdot 10^4$ kG/cm. As the beam has tiny cross section, the radius of aperture A of the quads can be also made small enough, providing high gradient G with small value of the pole field H as $G \cong H/A$. If we estimate $H \cong 15$ kG, $A = 0.01$ mm (20 μm in dia of aperture), then we come to gradient required $G \cong 1.5 \cdot 10^4$ kG/cm. At higher energy the actual emittance becomes adiabatically lower and the envelope function value allowed to be increased.

Thus, the focusing with the quadrupole lenses only is acceptable for the laser wavelength about 10 μm , what defines the transverse dimensions of the grating.

RF focusing occurs if the particle is going out of the RF crest [20]. If $x, y = 0$ the net force on the particle can be represented in the form

$$\langle F_x \rangle \cong \frac{e\mathcal{E}_z}{2w^2} \text{Sin}\phi \cdot x, \quad \langle F_y \rangle \cong -\frac{e\mathcal{E}_z}{2w^2} \text{Sin}\phi \cdot y, \quad (14)$$

where \mathcal{E}_z is the amplitude of the longitudinal (accelerating) field in the groove, ϕ is the RF phase (at the crest of RF $\phi = 0$). These forces are the quadrupole type for the particles out of the crest of RF. The effective factor of the lens can be evaluated as

$$k_x = -\frac{1}{pc} \frac{\partial \langle F_x \rangle}{\partial x} \cong \frac{e\mathcal{E}_z}{2mc^2 w^2} \text{Sin}\phi, \quad k_y = -\frac{1}{pc} \frac{\partial \langle F_y \rangle}{\partial y} \cong \frac{e\mathcal{E}_z}{2mc^2 w^2} \text{Sin}\phi. \quad (15)$$

Substitute here $\lambda = 10\mu\text{m}$, $\gamma = 2 \cdot 10^4$ ($pc = 10$ GeV), $w = 5\mu\text{m}$, $\mathcal{E}_z = 10^4 \text{V/m}$, we obtain $k_x = 2 \cdot 10^3 \cdot \text{Sin}\phi [\text{m}^{-2}]$. There are proposals to use this force for alternating phase focusing (APF), when the phase of the beam with respect to the RF crest is periodically

changed, $\phi = \pm\phi_0$ [21]. In our case this can be made by arranging periodical delay of the accelerating light arriving to the grating, for example, by modulation of the thickness of the lens 7 in Fig. 9. Anyway one can see that the RF focusing could be, in principle, two orders of magnitude more strong, than one uses a conventional quad, scaled to appropriate level.

Simplest Foxhole structure focuses the beam in horizontal direction [13]⁷. The possible scheme also is that the RF focusing arranged by the slots of the structure in horizontal direction and vertical focusing made by quadrupoles. This can reduce the betatron wavelength, in principle, two times. Different dimensions of the beam according to variation of the envelope function make it possible to adjust the focusing slots sequence to this variation.

9. Accelerating gradient

Let us suggest that full energy carried by a laser bunch is Q . For a time duration τ (see Fig. 1.2), we conclude, that the number n of periods in the bunch is about $n = \tau/T = c\tau/\lambda$, where $T = \lambda/c$ is a period of radiation. So, the field energy stored in the volume corresponding to a half of period is $W_g \cong Q/2n$. From the other side $W_g \cong (1/2)\epsilon_0 E_z^2 V_g$, where ϵ_0 is the dielectric permeability of the vacuum, $V_g \cong gW/g\lambda^2$ (W from Fig.8) is the effective volume, where the energy is concentrated. From the expressions for W_g , one can obtain the maximal field strength

$$E_{\text{max}} \cong \sqrt{Q/(e \cdot \tau \cdot \lambda \cdot g)} \quad (16)$$

For estimation let us take $Q = 0.01$ J, $\tau \cong 0.1$ ns, $\lambda \cong 1\mu\text{m}$, $g \cong \lambda/2 = 0.5\mu\text{m}$. This gives the field strength $E_{\text{max}} \cong 270$ GeV/m. This value must be reduced by the factor, taking into account the longitudinal length l_z instead of g , see Fig.1.2. The longitudinal length could be estimated as a $l_z = L/N_g$, where L is the length of the structure. For $\lambda \cong 1\mu\text{m}$ one can expect $N_g = 100$, so the length of our interest is $l_z = c\tau/N_g$, what is $l_z \cong 0.03\text{cm} \cong 300\lambda$. So the formula (16) must be rejected by factor $\sqrt{g/l_z} = 0.04$, what gives the field strength at the surface of the structure as high as $E_{\text{max}} \cdot \sqrt{g/l_z} = 10\text{GeV/m}$. The value of electrical field inside the structure could be found by taking into account RF quality factor Q_{str} , see section about accelerating structure. For $Q_{\text{str}} = 9$ it could reach again $E_{\text{max}} \cdot \sqrt{Q_{\text{str}} \cdot \sqrt{g/l_z}} = 30\text{GeV/m}$. The laser flash with $Q \cong 10$ mJ at $\lambda \cong 1\mu\text{m}$ is able to feed the accelerating structure with the length about $c\tau \cong 3\text{cm}$ with ≥ 30 GeV/m. A flash with $Q = 1$ J will feeds the 3 m total accelerating length, providing the energy gain $\cong 100\text{GeV}$. $Q = 100$ J could feed 10 TeV machine. Of course effective length of accelerator will be bigger, taking into account some filling factor reserved for focusing lenses, deflecting devices and so on.

⁷ The RF quadrupole focusing for both direction also may be arranged here as well. In this case the slots between the grooves has some modulations in the channel cross section [13].

For $\lambda \approx 10 \mu\text{m}$ the numbers are the following. First of all E_m from (16) is ten times lower. Number of resolved spots for electro-optical device is also lower, $N_s \approx 10-20$. But the factor $\sqrt{\delta/l} \approx \sqrt{\delta} N_s / c\tau$ about the same. So for the same Q_m factor accelerating gradient will be about 30 GeV/m for laser flash 10 mJ distributed along 3 cm length.

The damage level to the grating by a laser radiation is strongly correlated with the duration of illumination. In TLF method the energy about $Q \approx 10 \text{ mJ}$ effectively distributed on the area $S \approx W \cdot L$ in this time. So it gives density of energy falling on this area as high as $Q/S \approx Q/WL = Q/\lambda L = 3 \text{ J/cm}^2$ for $\lambda \approx 10 \mu\text{m}$ and 30 J/cm^2 for $\lambda \approx 1 \mu\text{m}$. Mostly of this energy reflected back. Widening the illumination area for $\lambda \approx 1 \mu\text{m}$ by factor of two will lower the power density to 15 J/cm^2 on expense of the gradient reduction down to $30/\sqrt{2} \approx 20 \text{ GeV/m}$. The illumination lasts for a time $t \approx l/c \approx l/c \approx 10^{-13} \text{ s}$. There are little of experimental data for the damage level, if illumination lasts for this time. Some scaling with the figures available shows, however, the possibility for $10^7 - 10^8 \text{ V/cm}$ without damage to the surface. The damaging level could depend on lot of factors, such as cleanliness, vacuum, temperature of accelerating structure⁸, technology of fabrication, heat treating and so on. So, the threshold limit is not a single number, it must reflect all conditions listed above.

We would like to stress here, that the TLF method itself does not avoid the problems associated with the breakdown limit. It allows to reach the field limit with the lowest energy of laser source. TLF method allows a drastic reduction of illuminating time also. As we mentioned, all these numbers allied with the number of resolved spots of deflecting device. In Table 2 we summarize the results of this chapter. Time duration $\tau \approx 100 \text{ ps}$.

	Power/Length	Gradient	Power density
$\lambda \approx 1 \mu\text{m}$	3 mJ/cm	30 GeV/m	30 J/cm^2
$\lambda \approx 10 \mu\text{m}$	3 mJ/cm	3 GeV/m	3 J/cm^2

Table 2.

10. Bunch population

The energy, accepted from the field by N particles is $W_s \approx eNE_m g(\delta)$ where e is the charge of a particle, $I(g)$ is a function of the order of unity - an analog of the transit time factor. The share of the energy will be

$$\eta W \approx \frac{1}{2} Q \lambda I(c\tau) \approx e N g(\delta) \sqrt{Q I(e c \tau \lambda \delta)} \quad (17)$$

From the last relation it follows that

$$N \approx \frac{\eta}{2 e I(\delta)} \sqrt{\frac{e \lambda^3 Q}{c \tau \delta}} \quad (18)$$

⁸ One can imagine the working temperature of liquid helium.

With $k(g) \approx 0.5$, $\eta \approx 0.05$ (5%), this yields $N \approx 1 \cdot 10^4$ for $\lambda \approx 1 \mu\text{m}$. For $\lambda \approx 10 \mu\text{m}$ this number will be $N \approx 3 \cdot 10^7$. As the length of the laser spot on the structure is $l_s \approx L/N_s$, what means that in principle, the number of the bunches could be

$$N_b \approx l_s / \lambda \approx L / N_s \lambda \quad (19)$$

Substitute here the numbers one can obtain $N_b \leq 300$ for $\lambda \approx 1 \mu\text{m}$, and $N_b \leq 100$ for $\lambda \approx 10 \mu\text{m}$.

If the final energy of the beam is E_b , repetition rate f Hz, then the total energy, caring by these particles per second is $\dot{E}_b \approx e N E_b f$. Substitute here $f = 160 \text{ Hz}$, $E_b = 300 \text{ GeV}$, we obtain $\dot{E}_b \approx e N E_b f = 16 \text{ J/sec}$, or 16 W . As we suggested the efficiency about 10%, the power of the laser must be at least 160 W for 160 Hz repetition rate. The impulse power of the laser is $P_l \approx Q/\tau$ and we have $P_l = 10^8 \text{ W}$ what is far below the limit achieved.

11. Wake and radiative instability

Mostly calculations for this type of structure done with of GARNET code [16]. The longitudinal and transverse wakes values normalized to one cell are $W_l \approx -7 \text{ kV/pC}$ and $W_t \approx 22 \cdot 10^3 \text{ V/pC}/\mu\text{m}$ correspondingly for the accelerating structure with $\lambda \approx 10 \mu\text{m}$, $\delta = 2 \mu\text{m}$, $w = 7 \mu\text{m}$ (see Fig.1) and the bunch with the longitudinal length $\sigma_l \approx 1 \mu\text{m}$ and bunch population $N \approx 10^4$. So the total charge is $eN \approx 16 \cdot 10^{-13} \text{ C}$ or 0.16 pC . A short wavelength of betatron oscillations helps against the resistive wall instability and wakefield influence reduction.

12. Final Focus

For realization the high luminosity the envelope function β^* in the interaction point must be of the bunch length value, what is about $0.1 + 1 \lambda$, i.e. $\sigma_l = \beta^* \approx 0.5 \mu\text{m}$. The envelope function value at the distance s from the interaction point will be, hence as big as

$$\beta = \beta^* + s^2 / \beta^* \approx s^2 / \beta^* \quad (20)$$

where we neglected the focusing, arising from incoming beam. With such an envelope function, the transverse dimension $\sigma_{t, \text{min}}$ will be of the order

$$\sigma_{t, \text{min}} \approx \sqrt{(\gamma e) \beta^* l \tau} \approx \sqrt{\frac{s^2}{\gamma \beta^*}} = \sqrt{\frac{(\gamma e)}{\gamma \beta^*}} \cdot s \quad (21)$$

For emittance we can take a (8a) value, $(\gamma e_s) \approx 1 \cdot 10^{-8} \text{ cm} \cdot \text{rad}$ what gives for energy $E \approx 17 \text{ TeV}$ ($\gamma \approx 2 \cdot 10^4$) the transverse dimension $\sigma_{t, \text{min}} \approx 0.1 \mu\text{m}$ for $s = 1 \text{ cm}$. Taking into account, that the angle, given to the particle by the field of the lens must be of the order of the natural angular spread in the focal point, $\sqrt{(\gamma e) / \gamma \beta^*} \approx G \cdot \sigma_{t, \text{min}} L_f / (HR)$, where L_f is the length of the lens, one can obtain [4d]

$$H_1 \approx G \sigma_{t, \text{min}} \approx \frac{(HR)}{FL_f} \sqrt{\frac{(\gamma e)}{\gamma \beta^*}} = \frac{(HR)}{L_f} \sqrt{\frac{(\gamma e)}{\gamma \beta^*}} \quad (22)$$

where we suggested, that the focal distance $F \approx s$. The length of formation the radiation is

$$l_r \equiv \rho / \gamma = L_r / \left(\gamma \cdot \sqrt{\frac{\gamma \epsilon}{\gamma \beta}} \right), \quad (23)$$

where $\rho \equiv (HR) / H_{\perp} = L / \sqrt{\epsilon / \beta}$ is the bending radius in the field of the lens. So the number of the radiated photons will be

$$N_r \equiv \alpha L / l_r = \alpha \cdot \gamma \cdot \sqrt{(\gamma \epsilon) / \gamma \beta}, \quad (24)$$

where $\alpha = e^2 / \hbar c$ - is the fine structure constant. As the critical photon energy is $\hbar \omega_c \equiv \frac{3}{2} \hbar \frac{c}{\rho} \gamma^3$, the total energy, radiated by the particle will be

$$\Delta E \equiv \hbar \omega_c \cdot N_r = \frac{3}{2} \hbar \alpha \frac{c \cdot \sqrt{\epsilon / \beta}}{L} \gamma \cdot \sqrt{\frac{\epsilon}{\beta}} \cdot \gamma^3 = \frac{3 e^2}{2 L} \gamma^4 \frac{\epsilon}{\beta} = \frac{3}{2} m c^2 \gamma^3 \frac{r_0 (\gamma \epsilon)}{L \beta}, \quad (25)$$

and the energy difference between the central particle and the particle at the boundary of the bunch will be

$$\frac{\Delta E}{E} \equiv \frac{3}{2} \gamma^2 \frac{(\gamma \epsilon) r_0}{\beta L}. \quad (26)$$

From the other side, variation of the focal distance due to energy variation is

$$\Delta F = -F \frac{\Delta E}{E} \equiv -\frac{(HR) 3}{GL} \gamma^2 \frac{\epsilon r_0}{\beta L}. \quad (27)$$

If we suppose that the focal distance is of the order of the length of the final lens, $F = L_r$, we came to final formula

$$\Delta F = -r_0 \gamma^2 (\gamma \epsilon) / \beta. \quad (28)$$

In our case $\Delta F = -2.8 \cdot 10^{-13} 4 \cdot 10^8 = 1.1 \cdot 10^{-4} \text{ cm}$ i.e. much bigger than the length of the bunch. So we came to fundamental conclusion [4d], that the final focus could not be arranged with help of single lens (or either a doublet) in case of focusing to the β required. The energy spread can be estimated as following

$$\delta(\Delta E) \equiv \hbar \omega_c \cdot \sqrt{N_r} = \hbar \frac{c}{L} \gamma^3 \sqrt{\alpha \gamma} \cdot \left(\sqrt{\frac{\epsilon}{\beta}} \right)^{3/2} \quad (29)$$

We suggested to arrange the final focusing for our purposes is a *multiplet* of FODO structures with the number of the lenses in multiplet of the order of few hundred [4d]. The gradient in these lenses must vary from the very strong at the side closest to IP, to weak at opposite side. Focusing properties of the RF lens, discussed above can be used here. A laser radiation of general and multiple frequency can be used for such focusing.

The laser radiation, phased with the main driving one can excite the single groove directly from the side. The quadrupole parameter described by (15). Substitute here $\lambda = 10 \mu\text{m}$, $\gamma = 2 \cdot 10^8$ ($pc = 1 \text{ TeV}$), $w = 5 \mu\text{m}$, $E_w = 10^8 \text{ V/m}$, we obtain $k_x = 4 \cdot 10^8 \cdot \sin \varphi [\text{m}^{-2}]$. For $\varphi = \pi/2$ this expression has a maximum. The variation of the focusing strength has a quadratic dependence with the deviation ψ from the angle $\varphi = \pi/2$, $k_x = \cos \psi$. For the longitudinal length of the groove about $g \equiv 5 \mu\text{m}$, the focal distance will be

$$F \equiv 1/k_g \equiv 1/4 \cdot 10^8 \cdot 5 \cdot 10^{-6} = 5 [\text{Meters/cell}]. \quad (30)$$

Equivalent gradient of the quadrupole lens is $G \equiv 0.3 \text{ pk} \equiv 1.2 \cdot 10^7 \text{ kGs/cm}$. So the lens with ≈ 500 cells having the length $L_r \equiv 0.5 \text{ cm}$ reaches the focal length $F \approx 1 \text{ cm}$.

For flattening the longitudinal dependence of the gradient (elimination the quadratic term in $k_x = \cos \varphi$ as a function of φ , see (14,15)), one can use the *second and higher harmonics* of the laser radiation, excited an additional groove, placed on the beam trajectory close to the first groove. For phasing, the highest harmonics can be generated by *multiplying* the frequency in nonlinear crystal. As initial, the splitted radiation from the general source (see Fig.13) can be used both for driving the first harmonic groove and, after doubling, the second one. For arranging a doublet of the focusing lenses, one can use the phase shift between the RF crest and the beam $\varphi = -\pi/2$. Such a tiny lens, not sensitive to detector magnetic field can be easily installed inside the detector.

13. Luminosity

For luminosity we have the formula

$$L \equiv \frac{N^2 f H_B \gamma \cdot N_B}{4\pi \sqrt{(\gamma \epsilon_x)(\gamma \epsilon_y)} \cdot \beta_x \beta_y}, \quad (31)$$

where H_B is the enhancement parameter. For emittances from (8 a, b) one can substitute here for $\beta_x = \beta_y = 0.3 \lambda$, $\lambda \equiv 10 \mu\text{m}$, $\gamma = 2 \cdot 10^8$ ($pc = 1 \text{ TeV}$), $N \equiv 2 \cdot 10^7$, $f \equiv 160 \text{ Hz}$, $H \equiv 2$, $N_B = 1$, $L = 1 \cdot 10^{33} \text{ cm}^{-2} \text{ s}^{-1}$. For $\lambda \equiv 1 \mu\text{m}$ result will be about the same as the number of the particles is lower here. The transverse size will be

$$\sigma_x \equiv \sqrt{(\gamma \epsilon_x) \beta_x} / \gamma \equiv \sqrt{10^{-8} \cdot 3 \cdot 10^{-4} / 2 \cdot 10^8} \equiv 1.2 \cdot 10^{-9} \text{ cm} = 0.12 \text{ \AA} \quad (32a)$$

$$\sigma_y \equiv \sqrt{(\gamma \epsilon_y) \beta_y} / \gamma \equiv \sqrt{4 \cdot 10^{-10} \cdot 10^{-4} / 2 \cdot 10^8} \equiv 1.4 \cdot 10^{-10} \text{ cm} = 0.024 \text{ \AA}. \quad (32b)$$

The effective longitudinal distance between the particles has the order $l_y / N = \lambda / N$. The last number in our case is formally $\leq 10^{-11} \text{ cm}$. As the distance $\approx \lambda_c \equiv 3.8 \cdot 10^{-11} \text{ cm}$ is absolute limit for such a spacing, we conclude that in each transverse slice $\approx \lambda_c$ the number of the particles $\approx 1-2$. The dimension (32b) formally corresponds to ≈ 4 particles per cross section.

Notice here that total length for acceleration up to 300 GeV could be about two tens of meters, taking into account that a fraction of the accelerating sections is of the order 50%. As the total energy of the full energy accelerator will be around 1 J , what gives the average power of the order 160 W .

The beams of electrons and positrons can be polarized what gives the effective gain in luminosity and reduces the background [23]. The possibility of operation with high repetition rate, up to *few kHz* is open.

14. Interaction point

For such a tiny dimensions one can expect a significant energy losses by synchrotron radiation in the interaction point. The Y_0 parameter which characterizes the radiation is

$$Y_0 = \frac{2 \hbar \omega_c}{3 E} = \gamma \frac{H}{H_c}, \quad (33)$$

where H is the magnetic field, $H_c = m^2 c^3 / e \hbar \approx 4.4 \cdot 10^{13} G$ is Schwinger critical field strength, ω_c is the critical frequency of classical synchrotron radiation. This parameter is a function of position inside the bunch. In our case magnetic field value H_0 in the longitudinal center of the bunch at its boundary can be estimated

$$H_0 \approx \frac{4\pi}{c} \frac{e N c}{2\pi \sigma_r \sigma_z} \approx 2.8 \cdot 10^{10} G, \quad (34)$$

so even for $E = 300 GeV$, $\gamma \approx 6 \cdot 10^5$, $Y_0 \approx 760$. It was taken into account that the electrical field of the incoming beam doubles the Y_0 . Thus the radiation is in a strong quantum regime. Energy losses for Gaussian bunch estimated in [22b]. For uniform transverse and Gaussian longitudinal distributions the Y parameter was represented as $Y = Y_0 \rho_1 \exp(-\zeta^2/2)$, where Y_0 calculated for the maximal field in the center of the bunch, $\rho_1 = r/\sigma_r$, $\zeta = z/\sigma_z$, are normalized coordinates. The normalized formation length parameter defined

$$F \approx F_0 \cdot \rho^{2/3} e^{\zeta^2} \approx \left(\frac{3}{2}\right)^{1/3} \frac{\lambda_c \gamma}{Y_0^{2/3} \sigma_r} \cdot \rho^{2/3} e^{-\zeta^2} = \left(\frac{3}{2}\right)^{1/3} \frac{\Gamma_0}{Y_0^{2/3}} \cdot \rho^{2/3} e^{\zeta^2}, \quad (35)$$

where $\Gamma_0 = \lambda_c \gamma / \sigma_r$.

The average fractional energy losses for strong quantum regime $Y_0 \gg 1$, described in first order by Sokolov-Ternov formula

$$\epsilon_s = \frac{\Delta E}{E} = \frac{16 \cdot \Gamma(2/3) \cdot 3^{2/3}}{243} \cdot \alpha \cdot \frac{Y_0^{2/3}}{\Gamma_0} (\rho_1)^{2/3} \int_{-\infty}^{\infty} \exp(-\zeta^2/3) d\zeta = \alpha \langle F \rangle, \quad (36)$$

what has clear physical sense, that at the length of formation $= \alpha$ photons are radiated. For the parameters discussed above, $\Gamma_0 \approx 23$. Substitute the figures in (35) one can obtain that $F_0 = 0.0044$, so on the length of the bunch a lot of photons are radiated. At this point we terminate our estimation referring to [22a]. Here the interaction of the beams with the parameters $\sigma_r \approx 0.4 \mu m$, $\sigma_z \approx 2.5 \text{ \AA}$, $N \approx 1.2 \cdot 10^8$ was considered. In their case $Y_0 = 5094$. The quantum beamstrahlung average fractional energy loss was found around 10% for the beam with energy 5 TeV. In our case the number of the particles is 10^{-3} of considered there, but the cross section is 10^2 times smaller. So the peak magnetic field is about the same. The radiation processes required more detailed considerations, however.

15. Multi-bunch operational mode.

Using a train of bunches (up to 100, see above) one can decrease the number of the particles in each bunch and/or to increase the cross section of the beam, thereby allow some reasonable losses. The length of the laser spot at the structure is about $l_l \approx L/N_b$, what we estimated in section 9 as $l_l = 0.03 cm$ what is $\approx 30\lambda$ for $\lambda \approx 10 \mu m$ and $\approx 300\lambda$ for $\lambda \approx 1 \mu m$. As the $Q_{RF} \approx 9$ required, then the number of the bunches could be 3-30. If collision arranged for few bunches per train, N_b , then the luminosity will get a gain factor

up to 3-30. These factors will allow to increase the transverse cross section and reduce the problems with radiation at IP. The H value required detailed considerations.

Multi-bunch structure could be arranged in a damping ring in principle with FEL methods. Using a laser with the same wavelength as required by acceleration structure and a dipole wiggler with period $\lambda_w \approx \lambda \cdot 2\gamma^2 / (1 + K^2)$ one can arrange an effective voltage $V \approx EKL_w / \gamma$, Where E is a laser field strength. Then the bunching could go with usual autophasing regime. For example if $E \approx 1 MV/cm$, $\gamma \approx 10^5$ (500 MeV), $L_w = 20m$, then effective voltage could reach $V \approx 2 MV$. Harmonics number (see section 7) could reach $q = \Pi / \lambda = 10^5 + 10^6$, where Π is a perimeter of the ring. According to section 7 this equivalent to 2 GeV of fundamental accelerating RF ($q=1$).

16. Alignment

The ratio of the random component of transverse momentum per stage Δp_{\perp} to the energy gained per stage Δp_{\parallel} must be less if compared with angular dispersion in the beam

$$\Delta p_{\perp} / p_{\parallel} \leq \sqrt{(\gamma\epsilon) / \beta\gamma} \quad (37)$$

Substitute here $\gamma\epsilon \approx 4 \cdot 10^{-10} cm rad$, $\beta \approx 10 cm$, $\gamma \approx 2000$ ($E \approx 1 GeV$, at the beginning of acceleration) we obtain $\Delta p_{\perp} / p_{\parallel} \approx 1.4 \cdot 10^{-7} rad$, for vertical and $\Delta p_{\perp} / p_{\parallel} \approx 7 \cdot 10^{-7} rad$ horizontal direction. From the other side $\Delta p_{\perp} / p_{\parallel} \approx \Delta\theta$, where $\Delta\theta$ is the accuracy of alignment of the grating. The $\Delta\theta$ can be

$$\Delta\theta \approx \Delta\phi \lambda / L \approx \Delta\phi \lambda / L \approx \Delta\phi \cdot 10^{-3} / 3 = 3 \cdot 10^{-4} \Delta\phi, \quad (38)$$

where $\Delta\phi$ is the phase resolution, if a diffraction methods of alignment are used. Compare the last expression with (37) one can conclude, $\Delta\phi \cdot \lambda / L \leq \sqrt{(\gamma\epsilon) / \beta\gamma}$ and required resolution is expected to be $\Delta\phi \approx 10^{-3}$ is big enough to be registered. The structure could be installed on the tables, moved by piezoelectric. Alignment *in situ* is going with help of radiation reflected from the structure. Adaptive optics could be used here as well.

17. General picture

As the system deals with the extreme bunches, a lot of feedback elements pursuit the beam's fluctuations. So that is why we suggest that both beams, the laser and particle's bunch go first to the end of all linear system apart from central station. On the way forward the bunch's (both, optical and particle's) parameters picked up, processed with appropriate algorithms and applied to correcting elements. Simplified view of such an assembly is represented in Fig. 11. All elements are placed in vacuumed volume, not show in this figure. Cross section of a tunnel with accelerating system shown in Fig. 12. All elements have a clear functional meaning, described in figures' capture. We supposed that the tunnel has a thermal stabilization of internal atmosphere. The duct 11 is a part of this system. A rack for control electronics and deflecting devices is shown as 8. Other elements, not marked in the capture are the water, vacuum and possible cryogenics ducts. Vacuumed tube 9 holds the Fresnel lenses for preliminary alignment (similar what are used at SLAC).

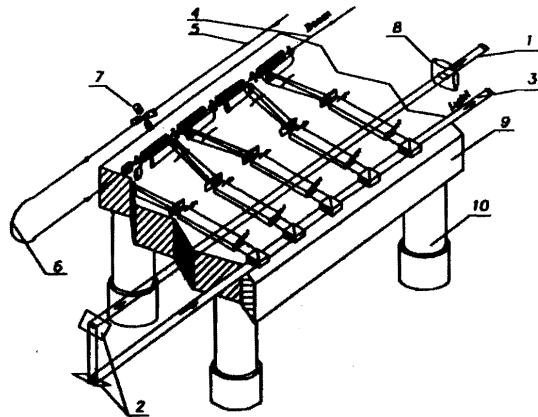


Fig. 11. Primary laser beam 1 goes to the end of accelerator. Mirrors 2 redirect it back, pos.3, through the sequence of splitters. In the similar way the particle's beam 5, goes through bending system 6 and further through structures to next modules, 4. 7 and 8— are the focusing elements for the laser and particle's beam correspondingly. Optical platform 9 is standing on legs 10 with active damping system to minimize vibrations.

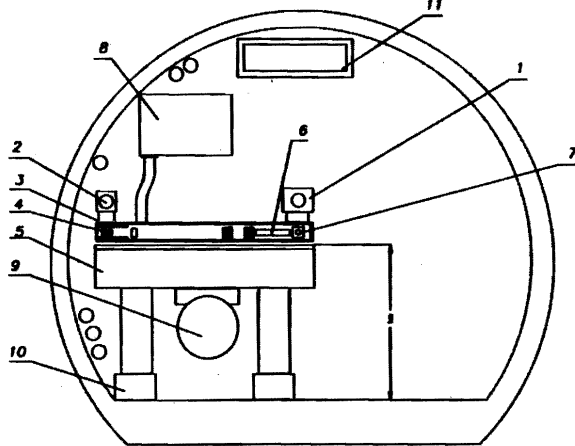


Fig. 12. Cross section of a tunnel with accelerating system. 1 is a primary optical beam line. 2—is primary particle's beam line. 3—is a vacuumed container with all equipment. 4—is an accelerating structure with sub systems. 5—is an optical table. 6—is deflecting device, 7—is a line for driving optical beam, 8—is a box with equipment for deflecting device and control. 9—is a tube with optical elements for active alignment of all optical tables. 10—is anti-vibration active system. 11—is a duct for air conditioning.

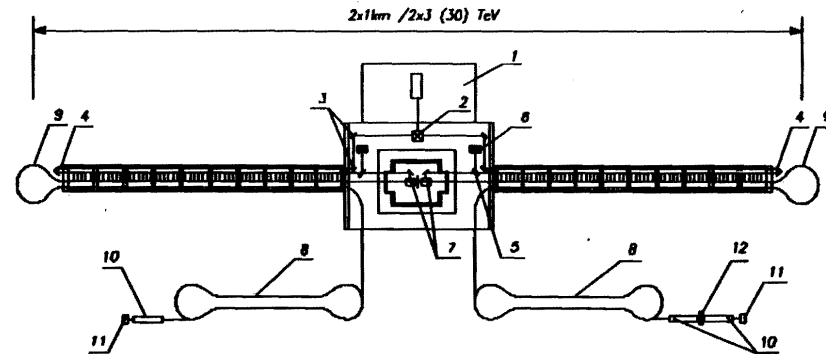


Fig. 13. Linear Laser Collider (LLC) complex. 1—is a laser platform, 2—is an optical splitter, 3,4—are the mirrors, 5 is a semi-transparent mirror, 6—is a light absorber. 7—are the Final Focus Systems. 8—are the damping rings for preparing particle's beams with small emittances, 9—are the bends for particle's beam. 10—are the accelerating S-band structures, 11—is an electron gun, 12—is a positron converter. Beam dump system is not shown.

General view of Linear Laser Collider (LLC) complex is represented in Fig.13. In figure capture all sufficient elements are mentioned. What is important here—to keep all final elements at both sides on the same stabilized platform to avoid affectation by vibration. Positioning the final stage of laser amplifier on the same platform is desirable for the same reason.

Table 3.

Parameter	$\lambda \cong 10\mu m$	$\lambda \cong 1\mu m$
Energy of e^{\pm} beam	$3 \times 3 TeV$	$30 \times 30 TeV$
Total two-linac length	$2 \times 1 km$	$2 \times 1 km$
Main linac gradient	$3 GeV/m$	$30 GeV/m$
Luminosity/bunch	$\leq 1 \cdot 10^{33} cm^{-2} s^{-1}$	$\leq 1 \cdot 10^{33} cm^{-2} s^{-1}$
No. of bunches/pulse	$3 (\leq 100)^*$	$10 (\leq 300)^*$
Laser flash energy/Linac	300J	300J
Repetition rate	160 Hz	160 Hz
Beam power/Linac	2.3 kW	760W
Bunch population	$3 \cdot 10^7$	10^6
Bunch length	$1\mu m$	$0.1\mu m$
$\gamma e, I \gamma e,$	$10^{-8} / 4 \cdot 10^{-10} cm \cdot rad$	$5 \cdot 10^{-9} / 1 \cdot 10^{-10} cm \cdot rad$
Damping ring energy	0.7 GeV	0.7 GeV
Length of section/Module	3cm	3cm
Wall plug power**	$2 \times 0.5 MW$	$2 \times 0.5 MW$

* -Maximal possible number . ** -Laser efficiency = 10%

In Table 3 we summarized the parameters of LLC. The parameters are represented for two different laser wavelengths. One can imagine, however, that LLC has two stages with these two wavelengths. Two types of lasers required for this obviously.

In this Table the power for supplemental electronics is not included.

A small *crossing angle* required to prevent illumination the final lenses by used beam. This angle is absolutely necessary for multi-bunch operational mode. Tiny dimensions of the beam can help to push the beams through with ordinary optics. Relatively low repetition rate, even few kHz, allows easily manipulate with the beams. Full energy in the laser flash distributed in the volume $\approx L_{acc} \cdot \lambda^2$, so $Q \approx E_e^2 \cdot L_{acc} \cdot \lambda^2$, where $L_{acc} -$ is a total length of accelerator. As we keep energy of the flash constant, $E_e \cdot L_{acc} = \frac{1}{\lambda} \sqrt{Q} \cdot L_{acc}$. That is why the final energy for $\lambda \approx 10 \mu\text{m}$ is ten times lower:

18. Perspectives

TLF method promises up to 30 TeV/m or 300 TeV on 10 km with 0.3 J/m or with 3 kJ per pulse total. So the total output power of the laser must be within 0.5 MW with repetition rate about 160 Hz for $\lambda \approx 1 \mu\text{m}$. Nd:Glass laser can be used here. CO₂ laser based system gives lower final energy, but the power required is within routinely obtained.

The gradient still far below the absolute limit of the acceleration gradient, what is defined by Schwinger field $eE^2 \approx mc^2/\lambda_c$. $E^2 \approx 10^{16} \text{ GeV/m}$, or 10^{18} TeV on 10 km.

19. Conclusions

Any point of accelerating structure must be illuminated for the minimal time in order to avoid the damage associated with the overheating. Greater accelerating gradient requires higher power density of radiation at the structure. *Traveling Laser Focus*, TLF, method solves both problems. Illuminating time and total laser power (or the flash energy) both defined by the number of resolved spots (pixels) associated with a deflecting device.

As the deflecting device must operate with 100 ps light bunches, the *traveling wave* regime is required for this device. Number of resolved spots $\approx 20 - 100$ achievable.

Due to the beam emittance available, the laser driven linac with $\lambda \approx 10 \mu\text{m}$ wavelength preferable from the point of *present day* workability.

The necessity to obtain the beta function at Interaction Point (IP) region below 1 μm requires very strong focusing, what can be arranged with RF lenses.

The electromagnetic collisions at IP are going in deep quantum regime and require additional considerations. A multi-bunch regime can diminish the problems associated with radiation. Repetition rate is another extensive parameter for further increase of luminosity with rejected bunch population.

Polarization of colliding beams could be a crucial issue in reduction of electromagnetic background at IP.

Lasers for the TLF method need to have more power in intermediate time duration $\tau \approx 100 \text{ ps}$ rather than increase the power in a shorter time interval. Equivalent time of illumination of accelerating structure with TLF is $0.1 + 1 \text{ ps}$.

The general conclusion is that TLF method reduces all requirements for Laser driven Linac to a present day front technology.

In conclusion author thanks M. Tigner and Yu. Orlov for their attention to this work.

20. References

- [1] Y. Takeda, IMAJMI, NIMM, 62(1968), p.306.
- [2] R.B. Palmer, Particle Accelerators, vol. 11, p.81, 1980.
- [3] I.V. Pogorelsky, et. Al. "The First Terawatt Picosecond CO₂ Laser for Advanced Accelerator Studies at the Brookhaven ATF", 7 Advanced Accelerator Concepts Workshop, 12-18 October 1996, Granlibakken, Lake Tahoe, CA, AIP 398 Proceedings, p.937.
- [4] a) A.A. Mikhailichenko, "The method of acceleration of charged particles", Author's certificate USSR N 1609423, Priority May 1989, Bulletin of Inventions (in Russian), №, p.220, 1994.
b) A.A. Mikhailichenko, "Excitation of the Grating by Moving Focus of the Laser Beam", EPAC 94, London, Proceedings, p. 802.
c) A.A. Mikhailichenko, "A Beam Focusing System for a Linac Driven by a Traveling Laser Focus", PAC95, Dallas, TX, Proceedings, p. 784.
d) A.A. Mikhailichenko, "A concept of a Linac Driven by a Traveling Laser Focus", 7 Advanced Accelerator Concepts Workshop, 12-18 October 1996, Granlibakken, Lake Tahoe, CA, AIP 398 Proceedings, p.547.
- [5] C.L. Ireland, J.M. Ley, "Electrooptical Scanners" in "Optical scanning", Edited by G. Marshall, Marcel Dekker, Inc., 1991. See also further references there.
- [6] "Selected Papers on Laser Scanning and Recording", SPIE Vol. 378, Editor L. Beiser, 1985.
- [7] V.J.Fowler, J.Schlafel, Applied Optics, Vol.5, N10, 1657(1966).
- [8] F.S.Chan et. al., "Light modulation and Beam Deflection with Potassium Tantalate-Niobate Crystals, Journ. Applied Physics, Vol.37, N1, p.388(1966).
- [9] J.F. Lodgeitch, IEEE Spectrum, 45 (Feb. 1968), see also [5].
- [10] C.L. Olson, C.A. Frost, E.L. Patterson, J.W. Poley, IEEE Trans. of Nucl. Sci., vol. NS-30, N4, 1983, p.3189.
- [11] L. Baskmann, "Acousto-Optical Laser Recording" in [6], p.255.
- [12] J. Rosenzweig, A. Muruthi, C. Pellegrini, "A proposed Dielectric-Loaded Resonant Laser Accelerator", Phys. Rev. Lett. 74, 2467(1995).
- [13] R.C.Petrow, J.Chau, "Properties of the Foxtale Accelerating Structure", AIP Conference Proceedings, 279, 1992, p.212.
- [14] H.Henke, "nan Wave Linac and Wiggler structure", EPAC 94, London.
- [15] J. Kirchgasser et al. "Superconducting RF Activities at Cornell University", SRF 950908-13, Cornell, 1995, see also SRF 950714-05 and references.
- [16] W. Bruns, Gathall, TU Berlin, 1997.

